

Resolved Photon Contributions to Higgs Boson Production in $\gamma\gamma$ Collisions

M. A. Doncheski

*Department of Physics, Pennsylvania State University,
Mont Alto, PA 17237 USA*

Stephen Godfrey

*Ottawa-Carleton Institute for Physics
Department of Physics, Carleton University, Ottawa, Canada K1S 5B6
and
TRIUMF, 4004 Wesbrook Mall, Vancouver B.C. Canada V6T 2A3*

Abstract

We study single Higgs boson production in $\gamma\gamma$ collisions proceeding via the hadronic content of the photon. These processes complement previous studies of pair and single Higgs production at e^+e^- colliders. For SM Higgs masses of current theoretical interest, the resolved photon contributions are non-negligible in precision cross section measurements. The charged Higgs cross sections are not competitive with the $\gamma\gamma \rightarrow H^+H^-$ process and at best might offer some information about quark-Higgs couplings. Finally, resolved photon production of the heavier Higgs bosons, H^0 and A^0 of the MSSM, can probe regions of the SUSY parameter space that will complement other measurements. This last process shows some promise in SUSY Higgs searches and warrants further study.

PACS numbers: 12.15.Ji, 12.60.Cn, 14.70.-e, 14.80.-j

I. INTRODUCTION

One of the fundamental questions of the standard model (SM) of particle physics is the origin of electroweak symmetry breaking (EWSB) [1,2]. The simplest description of EWSB results in one neutral scalar particle, the Higgs boson, which has well known problems associated with it. A priori, a more complicated Higgs sector is phenomenologically just as viable. The next simplest case is the general two Higgs doublet model (2HDM). A constrained version of the 2HDM arises in the minimal supersymmetric extension of the SM (MSSM) [3] where spontaneous symmetry breaking is induced by two complex Higgs doublets and leads to five physical scalars; the neutral CP-even h^0 and H^0 bosons, the neutral CP-odd A^0 boson, and the charged H^\pm bosons. At tree level the MSSM Higgs sector has two free parameters which are usually taken to be the ratio of the vacuum expectation values of the two Higgs doublets, $\tan\beta = v_2/v_1$, and the mass of the A^0 boson, m_A . The elucidation of EWSB is the primary goal of the Large Hadron Collider at CERN (LHC).

Direct searches at LEP2 yield lower limits $M_H > 114.4$ GeV for the SM Higgs mass [4] and $M_{h,A} \gtrsim 90$ GeV for the neutral SUSY Higgs masses while $M_{H^\pm} \gtrsim 80 - 90$ GeV depending on the H^\pm decay modes. More detailed results have been presented by the LEP Collaborations as plots of excluded regions of the MSSM parameter space [4]. Similar plots have been obtained by the CDF and D0 collaborations at the Tevatron $p\bar{p}$ collider [5]. It is expected that Run II of the Tevatron $p\bar{p}$ collider will be able to find evidence at 3σ for the SM Higgs boson up to about 180 GeV although a 5σ signal is limited to around 130 GeV [6].

In proton-proton collisions at $\sqrt{s} = 14$ TeV at the LHC the ATLAS [7] and CMS [8] experiments have shown that they are sensitive to the SM Higgs boson over the entire mass range of 100-1000 GeV. The MSSM Higgs boson can be discovered in a variety of channels so that at least one Higgs boson can be discovered for the entire parameter range. In a fraction of the parameter space more than one Higgs boson is accessible. However, there is a region in which the extended nature of the supersymmetric Higgs sector may not be observable since only the lightest Higgs boson can be seen in SM-like production processes. Likewise, only a limited number of measurements of Higgs boson properties can be carried out at the LHC.

A future high energy linear e^+e^- collider has been proposed as an instrument that can perform precision measurements that would complement those performed at the LHC [9,10]. In this context, the photon-photon ‘‘Compton-collider’’ option, from backscattered laser light off of highly energetic and possibly polarized electron beams, has been advocated as a valuable part of the LC physics program [11]. Recently, a number of papers have shown how the Compton-collider option can make important measurements in the Higgs sector [12–18]. For example, the analysis by Mühleitner, *et al.*, shows that the $\gamma - \gamma$ option of TESLA can be used to produce the h^0 , H^0 , and A^0 for intermediate values of $\tan\beta$ that may escape discovery at the LHC [13,12].

In this paper we show that the hadronic content of the photon can result in cross sections large enough that they should be considered in precision measurements of $\gamma\gamma \rightarrow H$ cross sections and that they may be useful in the study of the Higgs sector of the theory. The importance of resolved photon contributions has been demonstrated by the OPAL [19] and DELPHI [20] collaborations in obtaining interesting limits on leptoquark properties from $e\gamma$

production of leptoquarks [21].

II. CALCULATIONS AND RESULTS

The resolved photon approach is the same for all processes we consider so we begin with a brief description of the generic approach shown in Fig. 1. In the resolved photon approach the quark and gluon content of the photon are treated as partons described by partonic distributions, $f_{q/\gamma}(x, Q^2)$ in direct analogy to partons inside hadrons [22]. The parton subprocess cross sections are convoluted with the parton distributions to obtain the final cross sections. However, since the photons themselves have an associated spectrum, either the energy distribution obtained from backscattering a laser from an electron beam [23] or the Weizsäcker Williams distribution [24], we must further convolute the cross sections with the photon distributions to obtain cross sections that can be compared to experiment. Thus, the cross sections are found by evaluating the following expression:

$$\sigma = \int dx_1 dx_2 dx_3 dx_4 f_{\gamma/e}(x_1, Q^2) f_{\gamma/e}(x_2, Q^2) f_{p_i/\gamma}(x_3, Q^2) f_{p_j/\gamma}(x_4, Q^2) \hat{\sigma}(\hat{s}) \quad (1)$$

where $p_{i(j)}$ represents parton $i(j)$ in the photon which could be a quark, anti-quark, or gluon, $\hat{\sigma}(\hat{s})$ represents the subprocess cross section with parton C of M energy $\sqrt{\hat{s}}$.

The processes we are studying are typically of the form $q\bar{q} \rightarrow h^0$ and therefore take a particularly simple form. In this preliminary study we only include tree-level contributions and are aware that higher order corrections are likely to be non-negligible. Nevertheless, we feel that our approach is satisfactory for a first survey of resolved photon contributions to identify which processes may warrant more detailed study. We will adopt the standard used in many LC studies that 20 events represents an interesting signal for the canonical integrated luminosities used in such studies of 1 ab^{-1} . We do not include branching ratios, detector efficiencies, nor consider backgrounds. In the former case the branching ratios are well known [25,26] and we assume that the environment is sufficiently clean that the signal can be reconstructed with reasonable efficiency. Clearly, our study is crude and a more detailed study is warranted which includes a realistic consideration of detector acceptance and efficiency assumptions, decays leading to final state particles, and background studies.

Our calculations have explicit dependence on the c and b -quark masses. We take $m_s = 0.15 \text{ GeV}$, $m_c = 1.4 \text{ GeV}$, $m_b = 4.4 \text{ GeV}$, $V_{cs} = 0.97$, and $V_{bc} = 0.04$ [27]. In addition, we used $M_W = 80.41 \text{ GeV}$, $G_F = 1.166 \times 10^{-5} \text{ GeV}^{-2}$, $\alpha = 1.0/128.0$, and $m_t = 175.0 \text{ GeV}$.

A. Standard Model Higgs Production

We begin with SM Higgs production because the discovery and elucidation of the standard model Higgs boson is the first order of business for any future collider project. One of the strongest motivations for the Compton collider is to measure Higgs boson properties. The 2γ production of the Higgs boson is an especially interesting reaction [12–14] as it proceeds via loop contributions [28] and is therefore sensitive to new particles much higher in mass than the CofM energy that cannot be produced directly. It has also been suggested that this reaction can be used to distinguish between the SM Higgs and the lightest scalar

Higgs of the MSSM in the decoupling limit in which no other Higgs or SUSY particles are observed at the LC [29]. It is therefore important that all SM contributions to this cross section be carefully considered.

The first process we consider is $q\bar{q} \rightarrow H$ where the quark and anti-quark arise from the quark parton distributions of the photon, the so called resolved photon processes. The expression for the subprocess cross section is rather trivial and is given by:

$$\sigma(q\bar{q} \rightarrow H) = \frac{G_F \pi}{3\sqrt{2}} m_f^2 \sqrt{(1 - 4m_f^2/M_h^2)} \delta(M_H^2 - \hat{s}) \quad (2)$$

The cross section is dominated by the c -quark content. The lower mass of the c -quark enters eqn. 2 quadratically, but its charge and mass enhance the c -quark content in the photon. In Fig. 2 we show, for the backscattered laser case with $\sqrt{s_{ee}} = 500$ GeV, 1 TeV and 1.5 TeV using the GRV distribution functions [30], the contributions from both $c\bar{c}$ and $b\bar{b}$ production and the sum of the two. We also show the cross sections for the subprocess $\gamma\gamma \rightarrow Ht\bar{t}$ [31] which we calculated using the COMPHEP computer package [32]. The contributions from lighter quarks (including the b) are dominated by the collinear region of $\gamma\gamma \rightarrow Hq\bar{q}$, and as such are well described via the resolved photon approach. On the other hand, due to its large mass, the t -quark avoids the collinear region so that the resolved photon approach is inappropriate and we use the full subprocess. For the Higgs masses we consider, this process is below threshold for $\sqrt{s_{ee}} = 500$ GeV due to the t -quarks produced. For $\sqrt{s_{ee}} = 1000$ GeV, where there is more available phase space, this mechanism is interesting for Higgs masses up to about 200 GeV and up to about 300 GeV for $\sqrt{s_{ee}} = 1500$ GeV. Whether these two cases are interesting experimentally will depend crucially on the t -quark tagging efficiency.

For comparison we also show the $\sigma(\gamma\gamma \rightarrow H)$ production which proceeds via loops. The expressions are well known in the literature [33,34] and we do not reproduce them here. Likewise, we show the contribution from gluon fusion, $\sigma(gg \rightarrow H)$, which arises from the gluon content of the photon. Again, the subprocess cross section is well known in the literature. A final process that will produce Higgs bosons is $\gamma\gamma \rightarrow HW^+W^-$ [35,36]. The cross section was calculated using COMPHEP [32] and is shown as the dot-dashed curves in Fig. 2. The cross sections are seen to be substantial, rivalling the dominant $\gamma\gamma \rightarrow H$ at $\sqrt{s_{ee}} = 1500$ GeV although it is much smaller at $\sqrt{s_{ee}} = 500$ GeV, where it is comparable to the resolved photon processes we are interested in. To some extent this process can be disentangled from the $\gamma\gamma \rightarrow H$ process and the resolved photon processes via W and jet tagging. Nevertheless it is yet another ingredient that should be considered in measuring the Higgs two-photon width.

The two photon process dominates the resolved photon processes over the full range of Higgs masses we consider. The gluon-fusion process is almost three orders of magnitude smaller than $\sigma(\gamma\gamma \rightarrow H)$ over the entire M_H range. We note that for $\sqrt{s} = 1500$ GeV the gluon-fusion contribution increases to about 10% of the total $q\bar{q}$ contributions for $M_H < 400$ GeV. This reflects the increasing importance of the small x contributions from the gluon distributions at higher \sqrt{s} . Nevertheless, it does not seem unreasonable to neglect the gluon fusion contributions in our results. In contrast, the quark annihilation processes contribute at the percent level for $M_H \sim 150$ GeV and $\sqrt{s_{ee}} = 500$ GeV. This increases to the several percent level for $\sqrt{s_{ee}} = 1.5$ TeV. This Higgs mass region has received considerable attention for study at a future Linear Collider and Compton Collider and measurements

of the $\gamma\gamma \rightarrow H$ cross section at this level of precision is touted as a probe of new physics entering via loops. Recent studies by Asner *et al* [16] and by Krawczyk *et al* [17] find that these processes can be measured to approximately the 2% level. Thus, depending on M_H , Higgs production via the hadronic content of the photon may not be negligible at this level of precision, suggesting that these contributions deserve further study.

There exist many different sets of photon parton distributions in the literature [22,37–40]. In Fig. 3 we give an indication of the uncertainties due to the distribution functions by plotting the variation in cross section using different photon parton distribution functions. The solid band and shaded bands are for $\sigma(c\bar{c} \rightarrow H)$, $\sigma(b\bar{b} \rightarrow H)$, and $\sigma(gg \rightarrow H)$ using the DO [37], GRV [30], DG [38], LAC1 and LAC2 [39] distributions. This, by no means represents a complete survey of available distributions and is only meant to illustrate the uncertainties inherent in our current knowledge. It can be seen that there is considerable variation in the cross section depending on the specific distribution used. Fortunately, with significant amounts of new data from the LEP and HERA experiments, revised distributions based on these new data are arriving [41]. To take a conservative approach we used the GRV distributions which generally give the smallest cross sections.

In addition to the Compton Collider configuration, $\gamma\gamma$ luminosities arise at $e\gamma$ and e^+e^- colliders. In $e\gamma$ collisions one γ comes from a backscattered laser as before, while the second photon is a Weizsäcker-Williams bremsstrahlung photon. In e^+e^- both photons are Weizsäcker-Williams photons. The Weizsäcker-Williams photon spectrum is softer than the backscattered laser spectrum but it extends to higher $x = E_\gamma/E_e$. In Fig. 4 we show the SM Higgs production cross section as a function of M_H for the 3 cases. As we go from $\gamma\gamma$ to $e\gamma$ to e^+e^- the cross section decreases by about an order of magnitude in each case although at larger values of M_H , near the kinematic limit where the $\gamma\gamma$ luminosity goes to zero, the $\gamma\gamma$ luminosity extends further out for the $e\gamma$ and e^+e^- cases. We find similar patterns for charged Higgs production and the production of the heavier Higgs bosons of the MSSM model. We will therefore only show cross sections for the $\gamma\gamma$ case, although for completeness we mention results for the e^+e^- and $e\gamma$ cases when appropriate.

B. Charged Higgs Boson Production

Charged Higgs bosons arise naturally from the simplest extension of the SM: the introduction of a second Higgs doublet. Two variations of the two doublet model are discussed in the literature: In Model I, v_2 couples to both the u and d -type quarks and the other field decouples. In Model II, which arises in the MSSM, v_2 couples to the up-type quarks and v_1 to the down-type quarks. The ratio of these VEV's is one of the fundamental parameters of the theory; $\tan\beta \equiv v_2/v_1$. In this paper we restrict ourselves to model II. A charged Higgs boson will be difficult to find at the LHC if its mass is greater than ~ 125 GeV. This discovery reach is extended to almost $M_{H^\pm} \sim \sqrt{s}/2$ at an e^+e^- linear collider where they can be pair produced in the process $e^+e^- \rightarrow H^+H^-$ with a cross section which depends mainly on the H^\pm mass, dropping quickly near threshold due to P -wave suppression [42,43]. Charged Higgs bosons can also be pair produced in the process $\gamma\gamma \rightarrow H^+H^-$ [44] Given the interest in their properties, there have been a number of recent studies of single charged Higgs bosons at LC's [45–47]. If charged Higgs bosons were observed, cross section measurements could potentially give information about the underlying theory.

As before the subprocess cross section is rather straightforward to calculate and for $b\bar{c}$ fusion in Model II is given by:

$$\sigma(b\bar{c} \rightarrow H^-) = \frac{G_F \pi}{3\sqrt{2}} |V_{bc}|^2 \frac{(m_b^2 \tan^2 \beta + m_c^2 \cot^2 \beta)(M_H^2 - m_b^2 - m_c^2) - 4m_b^2 m_c^2}{\sqrt{(M_H^2 - m_b^2 - m_c^2)^2 - 4m_b^2 m_c^2}} \delta(M_H^2 - \hat{s}) \quad (3)$$

with an analogous expression for $s\bar{c}$ fusion. We include in our results a factor of 2 to take into account that the b -quark can come from either photon and likewise for the c anti-quark and a 2nd factor of 2 for summing over H^- and H^+ production. A priori one would expect the bc process to dominate over the cs process due to the much larger mass of the b -quark compared to the s -quark mass. However, the mass ratios m_s/m_b and m_c/m_b are compensated by the ratio of the CKM matrix elements V_{cs}/V_{cb} so that $m_s/m_b \times V_{cs}/V_{cb} \simeq 0.8$ and $m_c/m_b \times V_{cs}/V_{cb} \simeq 8$. For small values of $\tan \beta$ the cs fusion process will be larger than the cb fusion process. In addition to bc and cs fusion, charged Higgs bosons can also be produced via bt fusion. The t -quark is too heavy to be treated as a massless constituent of the photon so in this case we calculate the cross section for $b\gamma \rightarrow H^- t$. Although this last process will have a kinematic limit constrained by the Higgs and t -quark mass, below threshold it is the dominant contribution due to the large t -quark mass [48]. Above the $H-t$ threshold the relative importance of the cs and cb subprocesses is dependent on $\tan \beta$ via eqn 3.

The various contributions are shown in Fig. 5 for $\tan \beta = 3.0$ and 40 for $\sqrt{s_{ee}} = 500$ GeV. It should be noted that the cross sections for $\tan \beta = 1.5$ are larger than those for $\tan \beta = 3.0$. In all cases, for relatively low M_H , the largest contribution to the total charged Higgs production cross section comes from the tb contribution. As the Higgs mass increases the other contributions become dominant until the tb contribution goes to zero at the t - H kinematic limit. For small values of $\tan \beta$ the cs contribution is larger than the bc contribution while for large values of $\tan \beta$ the cs and cb contributions are comparable in size. In Fig. 6 we show the sum of these three contributions for a range of values of $\tan \beta$. For comparison, we also show the cross sections for $e^+e^- \rightarrow H^+H^-$ (medium dashed line) [43] and for $\gamma\gamma \rightarrow H^+H^-$ (dot-dashed line) [49,44].

Using the criteria adopted by the TESLA TDR of 20 events for 1 ab^{-1} of integrated luminosity we find that for $\sqrt{s_{ee}} = 500$ GeV, a charged Higgs bosons can be detected in this process up to $M_H = 270$ GeV and 240 GeV for $\tan \beta = 40$, and 30 respectively. As we have not taken into account acceptance cuts nor have we examined background reduction these numbers should be taken with a grain of salt. A proper analysis would require detailed simulations including detector dependent considerations which are clearly beyond the scope of the present work. With this caveat, for the high $\tan \beta$ cases, a charged Higgs boson could be detected with mass roughly comparable to the standard kinematic limit associated with charged particle pair production at e^+e^- colliders. However, these cross sections are greater than most of the processes considered by Kanemura, *et al.* [45] so that cross section information from this production mechanism would offer complementary information to other processes. For $\tan \beta > 1$, charged Higgs boson production in Model I would be too small to be observed.

We also considered the case where the photons bremsstrahlunged off of the incident e^+e^- beams using the Weizsäcker-Williams effective photon distribution. In this case the cross

sections would only produce measurable event rates for Higgs masses much smaller than could be produced in the pair production process $e^+e^- \rightarrow H^+H^-$. The intermediate case, for an $e\gamma$ collider, where one photon radiates off an initial beam electron and the other obtained from backscattering a laser off of the initial electron beam results in a cross section intermediate in magnitude between the $\gamma\gamma$ case and e^+e^- case. Using the same criteria as above, for $\sqrt{s_{ee}} = 500$ GeV we obtain measurable rates for $M_H < 145$ and 165 GeV for the $\tan\beta = 30$ and 40 cases. The discovery limits for various collider energies are summarized in Table I. Given that $\sigma(e^+e^- \rightarrow H^+H^-)$ is significantly larger than these cross sections it is unlikely that much would be learned from this process in $e\gamma$ collisions.

Motivated by the article of Kanemura, *et al.* [45], we also calculated the resolved photon contributions to $H^\pm W^\mp$ production which proceeds via $q\bar{q}$ fusion through an intermediate neutral Higgs boson. However, the cross sections were found to be small with event rates uninteresting from an experimental point of view.

C. Heavy MSSM Neutral Higgs Boson Production

In two Higgs doublet models there exist a total of three neutral Higgs bosons in addition to the two charged Higgs bosons discussed above. The three neutral Higgs bosons consist of two CP-even bosons, h and H , the former light and the latter heavy, and a heavy CP-odd boson A . At the CERN LHC, the pseudoscalar Higgs is not detectable above $M_A \gtrsim 250$ GeV for intermediate values of $\tan\beta$ [50]. The MSSM Higgs bosons can be produced in $\gamma\gamma$ collisions, $\gamma\gamma \rightarrow h^0, H^0, A^0$, with favorable cross sections allowing a heavy Higgs boson to be found up to 70-80% of the initial e^+e^- collider energy for moderate values of $\tan\beta$ [13]. However, it turns out that the resolved photon process has different dependence on $\tan\beta$ than the process proceeding through intermediate loops [51]. For example, the two-photon decay width of the A^0 is small for large $\tan\beta$ while the decay width of the H^0 is small for small $\tan\beta$ [25]. For the resolved photon processes, for large M_A the A^0 and H^0 have roughly similar cross sections independent of $\tan\beta$.

We use the minimal supersymmetric standard model (MSSM), to partially constrain the parameters of the model in our calculations [33,52]. Taking $\tan\beta$ and M_A or M_{H^\pm} as input, the rest of the parameters can be calculated. For simplicity, and given the other uncertainties in our results, we use tree level relationships for the various parameters. These are given by:

$$\begin{aligned}
M_{H^\pm}^2 &= M_A^2 + M_W^2 \\
M_{H^0, h^0}^2 &= \frac{1}{2}[M_A^2 + M_Z^2 \pm \sqrt{(M_A^2 + M_Z^2)^2 - 4M_Z^2 M_A^2 \cos^2 2\beta}] \\
\cos 2\alpha &= -\cos 2\beta \left(\frac{M_A^2 - M_Z^2}{M_H^2 - M_h^2} \right)
\end{aligned} \tag{4}$$

The Higgs couplings to quarks are given by:

$$\begin{aligned}
h^0 c\bar{c} &: \frac{-igm_c \cos \alpha}{2M_W \sin \beta} \\
h^0 b\bar{b} &: \frac{igm_b \sin \alpha}{2M_W \cos \beta}
\end{aligned}$$

$$\begin{aligned}
H^0 c\bar{c} &: \frac{-igm_c \sin \alpha}{2M_W \sin \beta} \\
H^0 b\bar{b} &: \frac{-igm_b \cos \alpha}{2M_W \cos \beta} \\
A^0 c\bar{c} &: \frac{-gm_c \cot \beta}{2M_W} \gamma_5 \\
A^0 b\bar{b} &: \frac{-gm_b \tan \beta}{2M_W} \gamma_5
\end{aligned} \tag{5}$$

These couplings result in the following subprocess cross sections:

$$\begin{aligned}
\sigma(c\bar{c} \rightarrow h^0) &= \frac{G_F \pi}{3\sqrt{2}} m_c^2 \frac{\cos^2 \alpha}{\sin^2 \beta} \delta(M_h^2 - \hat{s}) \\
\sigma(b\bar{b} \rightarrow h^0) &= \frac{G_F \pi}{3\sqrt{2}} m_b^2 \frac{\sin^2 \alpha}{\cos^2 \beta} \delta(M_h^2 - \hat{s}) \\
\sigma(c\bar{c} \rightarrow H^0) &= \frac{G_F \pi}{3\sqrt{2}} m_c^2 \frac{\sin^2 \alpha}{\sin^2 \beta} \delta(M_H^2 - \hat{s}) \\
\sigma(b\bar{b} \rightarrow H^0) &= \frac{G_F \pi}{3\sqrt{2}} m_b^2 \frac{\cos^2 \alpha}{\cos^2 \beta} \delta(M_H^2 - \hat{s}) \\
\sigma(c\bar{c} \rightarrow A^0) &= \frac{G_F \pi}{3\sqrt{2}} m_c^2 \cot^2 \beta \delta(M_A^2 - \hat{s}) \\
\sigma(b\bar{b} \rightarrow A^0) &= \frac{G_F \pi}{3\sqrt{2}} m_b^2 \tan^2 \beta \delta(M_A^2 - \hat{s})
\end{aligned} \tag{6}$$

The cross sections for H^0 and A^0 production via $b\bar{b}$ and $c\bar{c}$ annihilation for $\tan \beta = 3$ and 30 are shown in Fig 7. For higher values of $\tan \beta$, $b\bar{b}$ annihilation dominates, while for lower values, $c\bar{c}$ annihilation becomes more and more important until at sufficiently small values of $\tan \beta$ the $c\bar{c}$ annihilation contribution will become larger than the $b\bar{b}$ contribution. Fig. 8 shows the sum of the $b\bar{b} \rightarrow H$ and $c\bar{c} \rightarrow H$ contributions for a variety of $\tan \beta$ values for $\sqrt{s_{ee}} = 500$ and 1000 GeV. For a $\gamma\gamma$ collider with $\sqrt{s_{ee}} = 500$ GeV, again using the criteria of 20 events for integrated luminosity of 1 ab^{-1} , the H^0 can be observed up to 375 GeV, 365 GeV, 275 GeV, 175 GeV and 135 GeV for $\tan \beta = 40, 30, 7, 3,$ and 1.5 respectively. The cross section is totally dominated by $b\bar{b}$ annihilation for the three large $\tan \beta$ cases while for $\tan \beta = 1.5$ the $c\bar{c}$ contribution is actually larger for the values of M_H with large enough cross section to allow for discovery. The relative importance crosses over for $M_H > 120$ GeV but for the full range of M_H shown, the $c\bar{c}$ contribution is not negligible.

The cross sections for A^0 production are very similar to the H^0 cross sections so we do not show them but simply summarize the results in Table II.

For both H and A production, for the larger values of $\tan \beta$, the H^0 and A^0 will be produced in substantial numbers for masses substantially larger than $\sqrt{s}/2$. Even if one uses a much more stringent criteria for discovery than the one we have adopted here, we expect that the heavy Higgs bosons can be observed with relatively high masses. This is in contrast to the SM Higgs production where the resolved photon contributions are at best a non-negligible contribution that need to be understood in precision measurements. If H and

A were produced in sufficient quantity it is possible that the cross section could be used to constrain $\tan\beta$ in analogy to the proposal by Barger, *et al.* to use heavy Higgs productions to determine $\tan\beta$ [54]. Thus, the resolved photon contributions may very well play an important role in understanding the Higgs sector.

This can be seen most clearly by showing the regions of the $\tan\beta - M_A$ plot which can be explored via H and A production. Plots are given in Fig. 9 for $\sqrt{s_{ee}} = 500$ and 1000 GeV. Three regions are shown. Region 1 is for $\sigma > 0.1$ fb which would result in > 100 events for 1 ab^{-1} , region 2 is for $\sigma > 0.02$ fb which would result in > 20 events while in region 3 less than 20 events would be expected. The regions covered would complement measurements made in other processes.

III. CONCLUSIONS

The resolved photon contributions to two photon production of the SM Higgs boson is non-negligible for the more probable Higgs masses found in electroweak fits. Given that this process is touted as a sensitive probe of new physics via loop contributions it is important that the resolved photon contributions be understood at the same level as the loop contributions.

The resolved photon production of charged Higgs is unlikely to be an important production mechanism. At best, if M_{H^\pm} and $\tan\beta$ take on certain values, it may offer complementary information to other processes.

Resolved photon production of the heavy Higgs bosons in the MSSM are potentially the most interesting processes. They can be produced up to relatively high mass and in regions of MSSM parameter space that complements other measurements.

Our results motivate further study including decay modes, the hadronic final states and the backgrounds relevant to these single Higgs boson production processes.

ACKNOWLEDGMENTS

The authors thank Sally Dawson, Pat Kalyniak, Maria Krawczyk, Wade Hong, and Uli Nierste for useful comments and discussions. This research was supported in part by the Natural Sciences and Engineering Research Council of Canada. The work of M.A.D. was supported, in part, by the Commonwealth College of The Pennsylvania State University under a Research Development Grant (RDG).

REFERENCES

- [1] For a recent review see S. Dawson, ICTP Summer School in High-Energy Physics and Cosmology, Miramare, Trieste, Italy, 29 Jun -17 Jul 1998. [hep-ph/9901280].
- [2] M. Carena and H.E. Haber, hep-ph/0208209.
- [3] For reviews of the MSSM see P. Fayet and S. Ferrara, Phys. Rept. **32**, 249 (1977); H. P. Nilles, Phys. Rept. **110**, 1 (1984); H.E. Haber and G. Kane, Phys. Rept. **117**, 75 (1985); M. Drees, hep-ph/9611409; X. Tata, hep-ph/9807526.
- [4] ALEPH, DELPHI, L3 and OPAL Collaborations, The LEP working group for Higgs boson searches, LHWG Note 2002-01 (July 2002); T. Junk, Talk at the 5th International Symposium on Radiative Corrections, Carmel CA, Sept 11-15, 2000 hep-ex/0101015.
- [5] D0 Collaboration (B. Abbott et al.), hep-ex/9902028; CDF Collaboration (F. Abe et al.), Phys. Rev. Lett. **79**, 357 (1997).
- [6] Report of the Higgs working group of the Physics at Run II Supersymmetry/Higgs workshop, hep-ph/0010338. See also reference 2.
- [7] ATLAS Collaboration, ATLAS Detector and Physics Performance Technical Design Report. CERN-LHCC 99-14.
- [8] CMS Collaboration. CMS Technical proposal, CERN-LHCC 94-38.
- [9] TESLA Technical Design Report, Part III: Physics at an e^+e^- Linear Collider, Ed. R.D. Heuer, D. Miller, F. Richard, P.M. Zerwas (March 2001).
- [10] A recent review of Higgs boson studies is given by M. Battaglia and K. Desch, hep-ph/0101165.
- [11] V. Telnov, Int. J. Mod. Phys. **A13**, 2399 (1998) hep-ex/9802003.
- [12] J.I. Illana LC-TH-2000-002 (<http://www.desy.de/~lcnotes/>); J.F. Gunion and H.E. Haber, 1990 DPF Summer Study on High Energy Physics, Snowmass CO; D.L. Borden, D.A. Bauer and D.O. Caldwell, Phys. Rev. **D48**, 4018 (1993); M. Krämer et al., Z. Phys. **C64**, 21 (1994) G. Jikia and S. Sölder-Rembold, Nucl. Phys. Proc. Suppl. **82**, 373 (2000); I.F. Ginzburg, M. Krawczyk, P. Osland, hep-ph/0101208.
- [13] M. Mühlleitner, M. Kramer, M. Spira, P.M. Zerwas, Phys. Lett. **B508**, 311 (2001) [hep-ph/0101083]; M.M. Mühlleitner, hep-ph/0101177.
- [14] M. Melles, W.J. Stirling, V.A. Khoze, Phys. Rev. **D61**, 054015 (2000).
- [15] J.-Y. Guo, Y. Liao, and Y-P. Kuang, hep-ph/9912277.
- [16] D.M. Asner, J.B. Gronberg, and J.F. Gunion, hep-ph/0110320.
- [17] P. Niezurawski, A.F. Zarnecki, and M. Krawczyk, hep-ph/0208234.
- [18] Z. Fei, M. Wen-Gan, J. Yi, L. Xue-Qian, W. Lang-Hui, Phys. Rev. **D64**, 055005 (2001).
- [19] OPAL Collaboration, (Stefan Soldner-Rembold for the collaboration), Presented at International Conference on the Structure and the Interactions of the Photon (Photon 97) including the 11th International Workshop on Photon-Photon Collisions, Egmond aan Zee, Netherlands, 10-15 May 1997. hep-ex/9706003.
- [20] DELPHI Collaboration (P. Abreu et al.), Phys.Lett. **B446**, 62 (1999).
- [21] M.A. Doncheski, and S. Godfrey, Phys.Rev. **D49**, 6220 (1994); Phys.Rev. **D51**, 1040 (1995); Phys.Lett., **B393**, 355 (1997); Mod. Phys. Lett. **A12**, 1719 (1997).
- [22] Two recent reviews are: R. Nisius, Phys. Rept. **332**, 165 (2000); M. Krawczyk, A. Zembrzuski, and M. Staszal, hep-ph/0011083.
- [23] I.F. Ginzburg, *et al.*, Nucl. Instrum. Methods, **205**, 47 (1983); *ibid* **219**, 5 (1984); V.I.

- Telnov, Nucl. Instrum. Methods, **A294**, 72 (1990); C. Akerlof, Report No. UM-HE-81-59 (1981; unpublished).
- [24] C. Weizsäcker, Z. Phys. **88**, 612 (1934); E.J. Williams, Phys. Rev. **45**, 729 (1934).
- [25] A. Djouadi, M. Spira, P.M. Zerwas, Z. Phys. **C70**, 427 (1996); Phys. Lett. **B311**, 255 (1993); M. Battaglia, hep-ph/9910271.
- [26] J. Kalinowski, P.M. Zerwas, Z. Phys. **C70**, 435 (1996).
- [27] Particle Data Group, K. Hagiwara et al, Phys. Rev. **D66**, 010001 (2002).
- [28] L. Resnick, M.K. Sundaresan, and P.J.S. Watson, Phys. Rev. **D8**, 172 (1973); M.K. Gaillard and D.V. Nanopoulos, Nucl. Phys. **B106**, 292 (1976).
- [29] H. Haber, hep-ph/9505240; hep-ph/9707213; A. Djouadi, V. Driesen, W. Hollik, and J.I. Illana, Eur. Phys. J. **C1**, 149 (1998).
- [30] M. Glück, E. Reya and A. Vogt, *Phys. Lett.* **B222**, 149 (1989); *Phys. Rev.* **D45**, 3986 (1992).
- [31] K. Cheung, Phys. Rev. **D47**, 3750 (1993).
- [32] P. A. Baikov et al., Physical Results by means of CompHEP, in Proc. of X Workshop on High Energy Physics and Quantum Field Theory (QFTHEP-95), eds. B. Levtchenko, V. Savrin, Moscow, 1996, p. 101, hep-ph/9701412; E. E. Boos, M. N. Dubinin, V. A. Ilyin, A. E. Pukhov, V. I. Savrin, hep-ph/9503280.
- [33] J. F. Gunion, H. E. Haber, G. L. Kane and S. Dawson, *The Higgs Hunter's Guide*, Addison-Wesley, Redwood City, USA, 1990.
- [34] V. Barger and R. J. Phillips, *Collider Physics*, Addison-Wesley, Redwood City, USA, 1987.
- [35] K. Cheung, Phys. Rev. **D50**, 4290 (1994).
- [36] G. Jikia, Nucl. Phys. **B437**, 520 (1995).
- [37] D.W. Duke and J.F. Owens, *Phys. Rev.* **D26**, 1600 (1982).
- [38] M. Drees and K. Grassie, Z. Phys. **C28**, 451 (1985).
- [39] H. Abramowicz, K. Charchula, and A. Levy, *Phys. Lett.* **B269**, 458 (1991).
- [40] M. Drees and R. Godbole, *Nucl. Phys.* **B339**, 355 (1990); M. Glück, E. Reya and A. Vogt, *Phys. Rev.* **D46**, 1973 (1992); G. A. Schuler, T. Sjöstrand, Z. Phys. **C68**, 607 (1995); Phys. Lett. B **376**, 193 (1996).
- [41] F. Cornet, P. Jankowski, M. Krawczyk, A. Lorca, hep-ph/0212160.
- [42] J.F. Gunion, *et al.*, Phys. Rev. **D38**, 3444 (1988); A. Djouadi, J. Kalinowski, P.M. Zerwas, Z. Phys. **C57**, 569 (1993); A. Djouadi, J. Kalinowski, P. Ohmann, P.M. Zerwas, Z. Phys. **C74**, 93 (1997).
- [43] S. Komamiya, Phys. Rev. **D38**, 2158 (1988).
- [44] D. Bowser-Chao, K. Cheung, and S. Thomas, Phys. Lett. **B315**, 399 (1993) [hep-ph/9304290].
- [45] S. Kanemura, S. Moretti, and K. Odagiri, Presented at the Linear Collider Workshop 2000, October 24-28 2000, Fermilab USA, hep-ph/0101354; J. High Energy Phys. **02**, 011 (2001) [hep-ph/0012030].
- [46] S. Moretti, and S. Kanemura, hep-ph/0211055.
- [47] H.-J. He, S. Kanemura, and C.-P. Yuan, hep-ph/0209376; Phys. Rev. Lett. **89**, 101803 (2002).
- [48] M.A. Doncheski, and S. Godfrey, in preparation.
- [49] H.G. Blundell, S. Godfrey, G. Hay, E.S. Swanson, Phys. Rev. **C61**, 025203 (2000).

- [50] M. Spira, Fortschr. Phys. **46**, 203 (1998).
- [51] See also Ref. [15].
- [52] J.F. Gunion and H. Haber, Nucl. Phys. **B272**, 1 (1986); erratum **B402**, 567 (1993); Nucl. Phys. **B279**, 449 (1986).
- [53] C. Caso, *et al.*, Particle Data Group, Eur. Phys. J. **C3**, 1 (1998).
- [54] V. Barger, T. Han, J. Jiang, Phys. Rev. **D63**, 075002 (2001).

TABLE I. The charged Higgs masses (in GeV) corresponding to 2×10^{-2} fb and 10^{-1} fb cross sections.

\sqrt{s}	$\tan \beta$	30		40	
		2×10^{-2} fb	10^{-1} fb	2×10^{-2} fb	10^{-1} fb
500 GeV	$\gamma\gamma$	240	180	270	200
	$e\gamma$	145	80	165	105
800 GeV	$\gamma\gamma$	410	345	425	375
	$e\gamma$	270	155	305	195
1000 GeV	$\gamma\gamma$	540	455	560	490
	$e\gamma$	350	205	395	255
1500 GeV	$\gamma\gamma$	855	705	890	765
	$e\gamma$	525	305	605	385

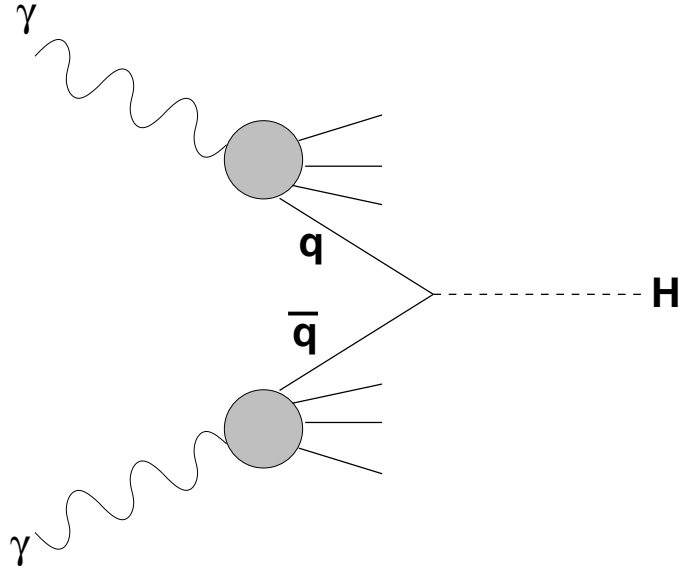


FIG. 1. Generic Feynman diagram for Higgs boson production via the resolved photon process $\gamma\gamma \rightarrow q\bar{q} + X \rightarrow H + X$.

TABLE II. The H^0 and A^0 Higgs masses (in GeV) corresponding to 2×10^{-2} fb and 10^{-1} fb cross sections.

\sqrt{s}	$\tan \beta$	σ (fb)	M_H					M_A				
			1.5	3	7	30	40	1.5	3	7	30	40
500 GeV	$\gamma\gamma$	0.02	135	175	275	365	375	125	180	275	365	375
		0.1	—	—	180	335	350	—	100	185	330	345
	$e\gamma$	0.02	—	—	125	275	295	—	—	135	270	295
		0.1	—	—	—	190	220	—	—	—	190	220
	e^+e^-	0.02	—	—	—	140	165	—	—	—	140	160
		0.1	—	—	—	—	100	—	—	—	—	100
800 GeV	$\gamma\gamma$	0.02	140	220	375	560	580	140	220	380	560	580
		0.1	—	—	230	480	520	—	115	220	475	510
	$e\gamma$	0.02	—	—	165	375	420	—	95	170	380	420
		0.1	—	—	—	250	295	—	—	95	250	390
	e^+e^-	0.02	—	—	—	195	225	—	—	80	195	220
		0.1	—	—	—	115	140	—	—	—	110	140
1000 GeV	$\gamma\gamma$	0.02	155	240	430	685	710	155	240	430	685	710
		0.1	—	100	240	560	610	—	120	250	570	620
	$e\gamma$	0.02	—	—	185	435	495	—	100	190	440	500
		0.1	—	—	—	280	330	—	—	100	280	340
	e^+e^-	0.02	—	—	—	220	255	—	—	—	220	255
		0.1	—	—	—	115	155	—	—	—	115	160
1500 GeV	$\gamma\gamma$	0.02	180	290	540	970	1020	180	280	530	960	1020
		0.1	—	140	290	750	840	100	150	300	760	830
	$e\gamma$	0.02	—	100	240	560	660	—	130	240	570	660
		0.1	—	—	120	360	430	—	—	130	360	440
	e^+e^-	0.02	—	—	—	280	315	—	—	—	250	300
		0.1	—	—	—	160	200	—	—	—	160	200

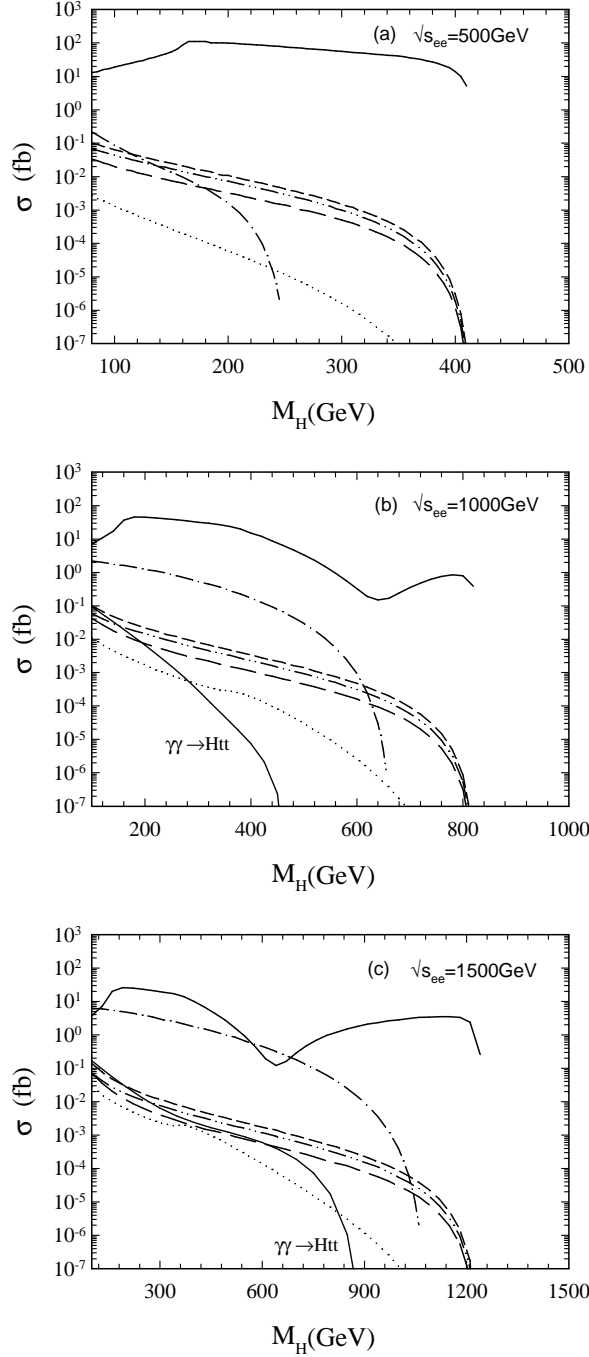


FIG. 2. Production cross sections for SM Higgs boson for (a) $\sqrt{s_{ee}} = 500$ GeV, (b) 1 TeV, (c) 1.5 TeV with backscattered laser spectrum. The solid line is for $\gamma\gamma \rightarrow h$, the short dashed line for $\hat{\sigma}(b\bar{b} \rightarrow h) + \hat{\sigma}(c\bar{c} \rightarrow h)$, the dot-dot-dashed line for $\hat{\sigma}(c\bar{c} \rightarrow h)$, the long-dashed line for $\hat{\sigma}(b\bar{b} \rightarrow h)$, the dotted line for $\hat{\sigma}(gg \rightarrow h)$ and the dot-dashed line for $\hat{\sigma}(WW \rightarrow H)$. $\sigma(\gamma\gamma \rightarrow Ht\bar{t})$ is shown by the labelled solid line.

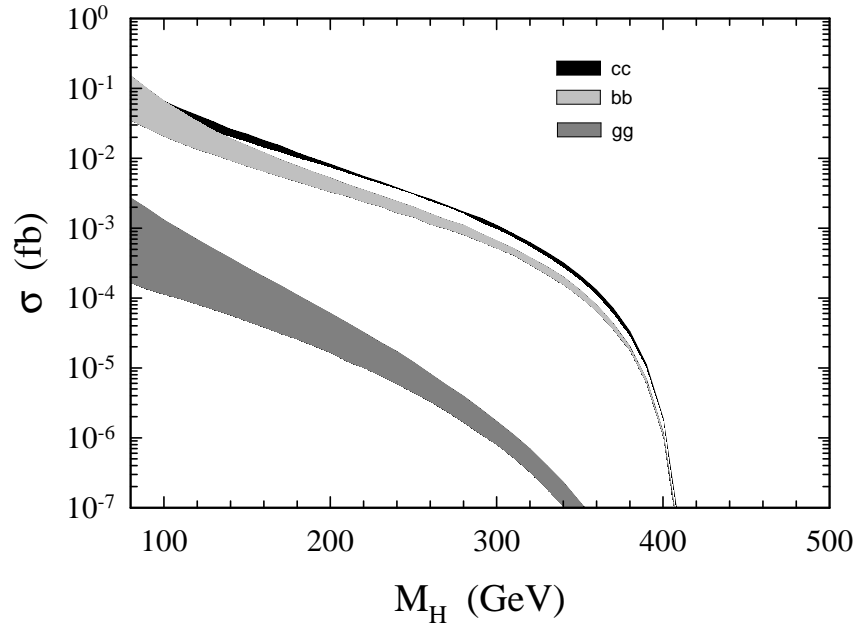


FIG. 3. Variation of the $\gamma\gamma \rightarrow H + X$ cross section using different parton distributions for $\sqrt{s_{ee}} = 500$ GeV with backscattered laser spectrum. Details are given in the text.

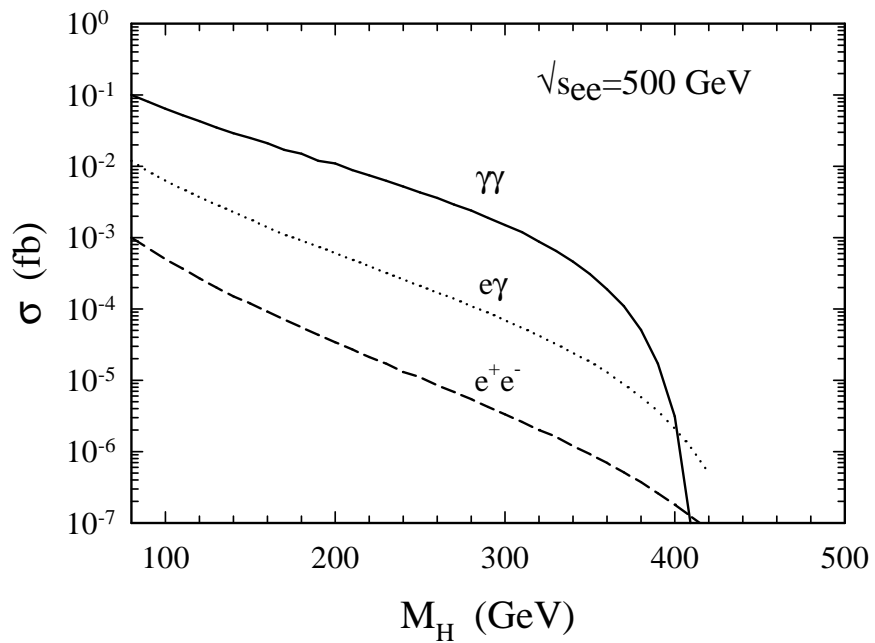


FIG. 4. SM Higgs production cross sections via resolved photons with $\sqrt{s_{ee}} = 500$ GeV. The solid line is for the $\gamma\gamma$ case, the dotted line for the $e\gamma$ case, and the dashed line for the e^+e^- case.

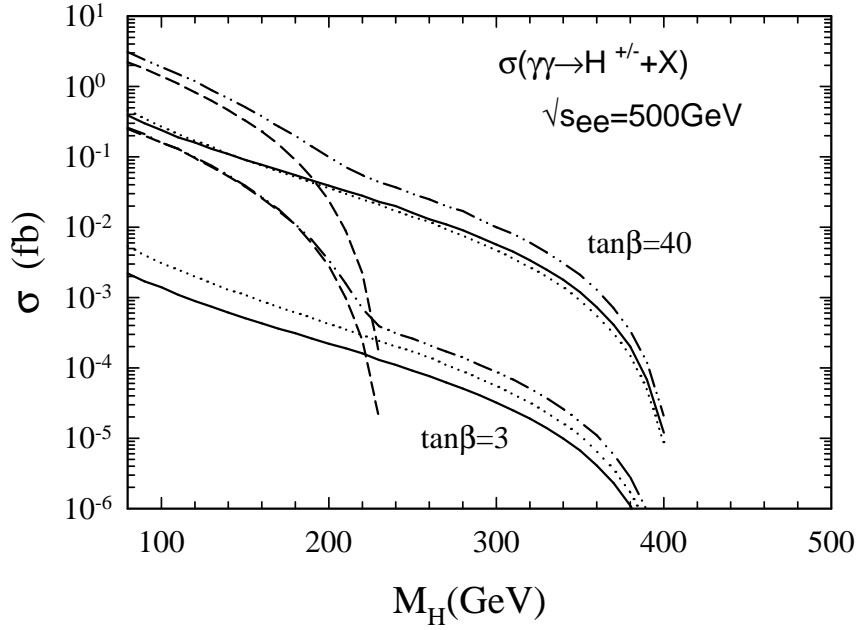


FIG. 5. Charged Higgs boson production via resolved photon contributions in $\gamma\gamma$ collisions at $\sqrt{s_{ee}} = 500$ GeV for $\tan\beta = 3.0$ and 40 . The solid lines are for cb -fusion, the dotted lines for cs -fusion, the dashed lines for the subprocess $\gamma b \rightarrow tH^{\pm}$ and the dot-dot-dashed lines for the sum of all three contributions to charged Higgs production.

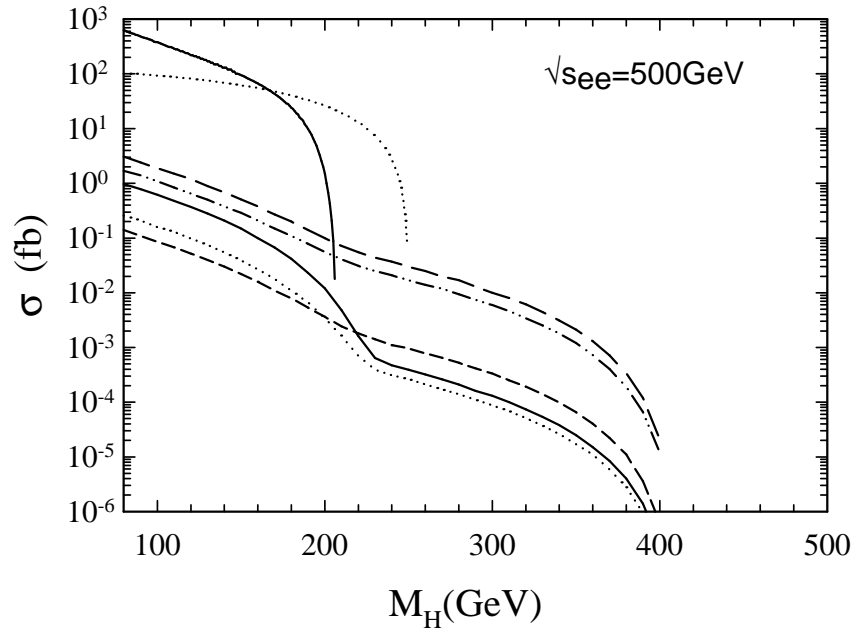


FIG. 6. Charged Higgs boson production via resolved photon contributions in $\gamma\gamma$ collisions at $\sqrt{s_{ee}} = 500$ GeV. The solid line is for $\tan\beta = 1.5$, the dotted line for $\tan\beta = 3$, the short-dashed line for $\tan\beta = 7$, the dot-dot-dashed line for $\tan\beta = 30$, the long-dashed line for $\tan\beta = 40$, the dot-dashed line for $\gamma\gamma \rightarrow H^+H^-$, and the medium dashed line for $e^+e^- \rightarrow H^+H^-$.

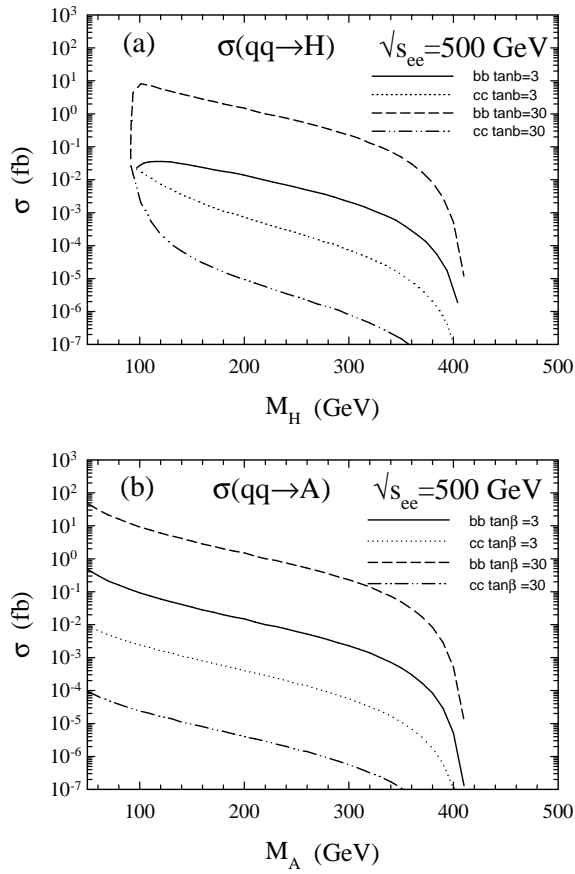


FIG. 7. Heavy MSSM Higgs boson production cross sections via resolved photons for $\sqrt{s_{ee}} = 500$ GeV with backscattered photons. (a) is for $\hat{\sigma}(q\bar{q} \rightarrow H)$ and (b) is for $\hat{\sigma}(q\bar{q} \rightarrow A)$. In both cases the solid line is for $\hat{\sigma}(b\bar{b} \rightarrow H(A))$ for $\tan\beta = 3$, the dotted line is for $\hat{\sigma}(c\bar{c} \rightarrow H(A))$ for $\tan\beta = 3$, the dashed line is for $\hat{\sigma}(b\bar{b} \rightarrow H(A))$ for $\tan\beta = 30$, and the dot-dot-dashed line is for $\hat{\sigma}(c\bar{c} \rightarrow H(A))$ for $\tan\beta = 30$.

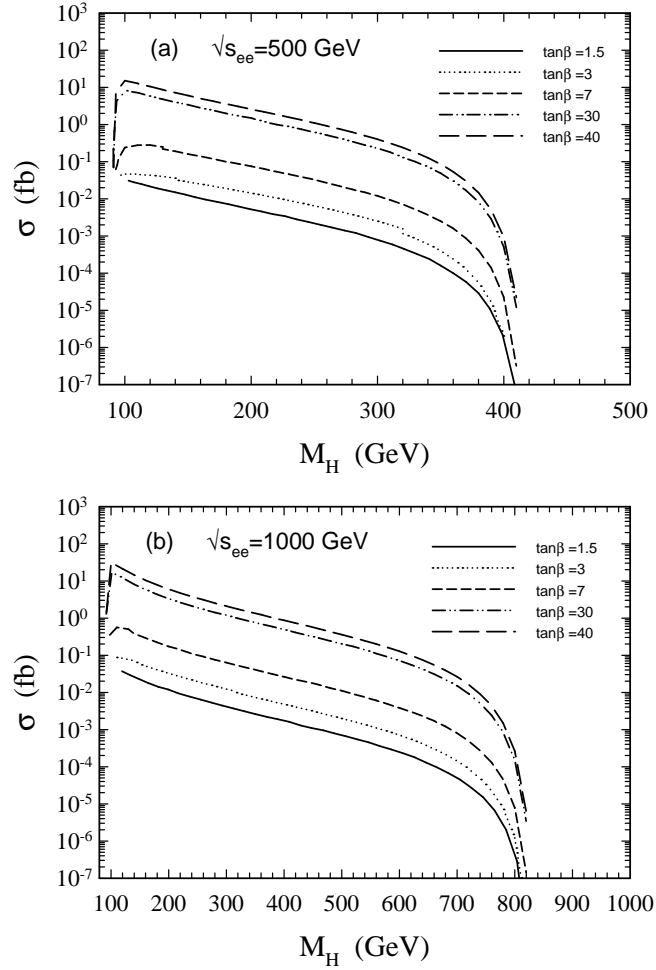


FIG. 8. H production cross sections via resolved photons for $\sqrt{s_{ee}} = 500$ GeV with backscattered photons from $\hat{\sigma}(c\bar{c} \rightarrow H) + \hat{\sigma}(b\bar{b} \rightarrow H)$. The solid line is for $\tan\beta = 1.5$, the dotted line for $\tan\beta = 3$, the short-dashed line for $\tan\beta = 7$, the dot-dot-dashed line for $\tan\beta = 30$, and the long-dashed line for $\tan\beta = 40$.

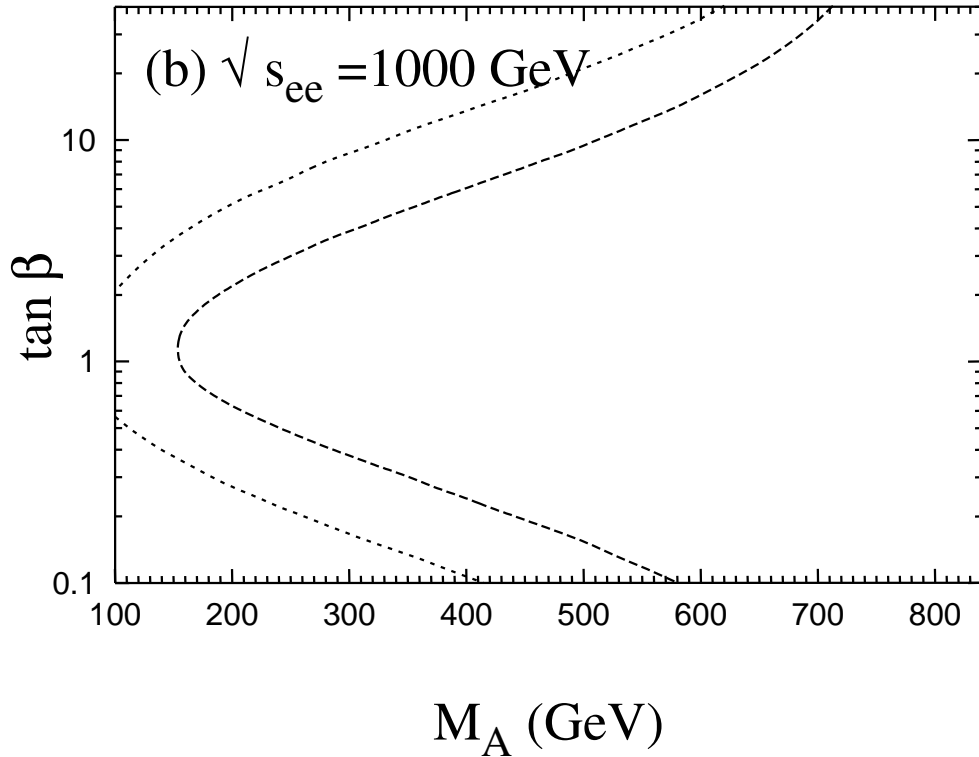
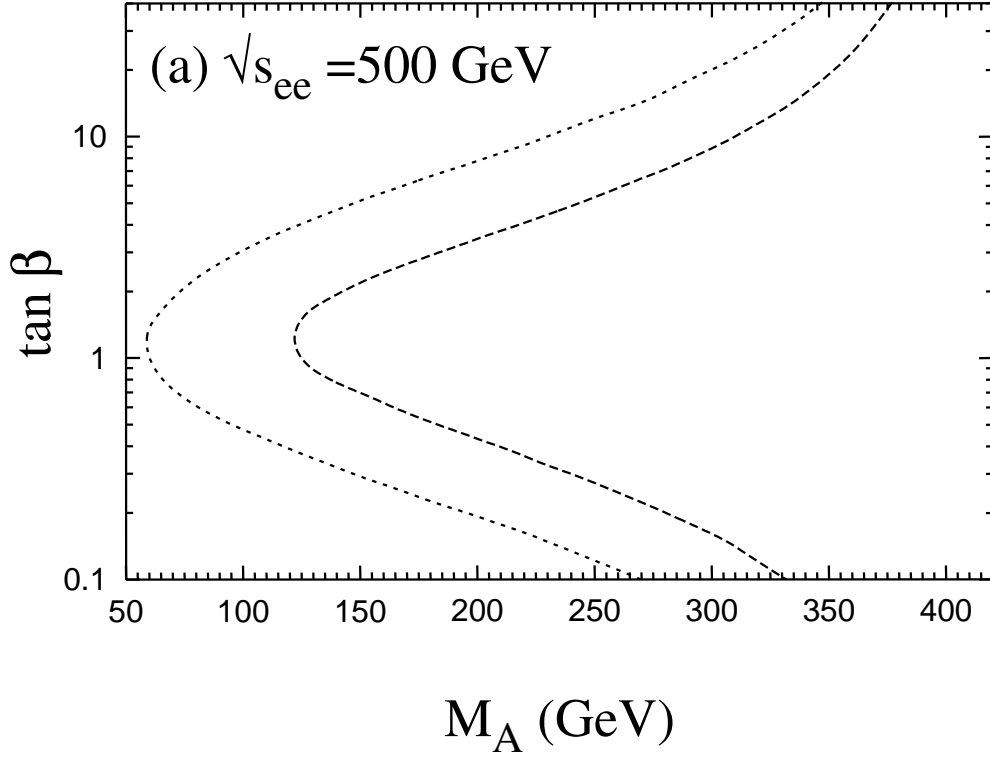


FIG. 9. Regions of sensitivity in $\tan \beta - M_A$ parameter space to A production via resolved photons with backscattered laser photons. The region to the left is accessible and the region to the right is unaccessible. The dotted line gives $\sigma = 0.1 \text{ fb}$ contour so that at least 100 events would be produced in the region to the left for 1 ab^{-1} integrated luminosity. Similarly the dashed line gives the $\sigma = 0.02 \text{ fb}$ contour designating the the boundary for producing at least 20 events. (a) is for $\sqrt{s_{ee}} = 500 \text{ GeV}$ and (b) for $\sqrt{s_{ee}} = 1000 \text{ GeV}$.